2-wavelength Beam Deflection Technique For Electron-density Measurements In Laser-produced Plasmas

Faris, G. W; Bergstrom, H

Published in:
Applied Optics

DOI:
10.1364/AO.30.002212

1991

Two-wavelength beam deflection technique for electron density measurements in laser-produced plasmas

Gregory W. Faris and Håkan Bergström

We describe the use of a two-wavelength beam deflection technique in the measurement of electron density and expansion velocity in a laser-produced plasma. Beam deflection measurements are made with a spatial resolution of 250 μm, temporal resolution of 25 ns, and a dynamic range of 1000. Several techniques for determining the spatial and temporal variation of the electron density from beam deflection measurements are described. *Key words:* Beam deflection, electron density, laser-produced plasma, two-wavelength two-color tomography, plasma expansion velocity.

I. Introduction

Laser-produced plasmas[1,2] and laser ablation are of current interest for a number of applications, including the production of atomic species of low vapor pressure species for spectroscopy[3] and new laser sources[4]; the production of clusters[5]; the production of VUV radiation[6] and soft x-ray radiation for optically pumping soft x-ray lasers,[7] for microscopy,[8] and for lithography[9]; collisional excitation of soft x-ray lasers[10]; deposition of diamond[11] and superconducting films[12]; and the etching of polymers.[13] Better understanding of these processes is assisted by useful diagnostic techniques for measuring parameters within the plasma. A simple plasma diagnostic that may be implemented with apparatus found in many laboratories is the beam deflection technique.

When a laser beam is passed through a region with varying index of refraction it is deflected by gradients in the index of refraction. The deflection angle α depends on the integrated gradient of the index of refraction and is given to a good approximation by[14]

$$\alpha(y) = \frac{1}{n_o} \int \frac{dn}{dy} dx, \tag{1}$$

where n is the index of refraction, n_o is the ambient index of refraction, x is the direction of the laser beam propagation, and y is the direction of the deflection. Measured deflection angles may be used to reconstruct the spatially resolved index of refraction in the probed region, which may then be related in various conditions to electron density,[3,15,16] gas density,[17] species concentration,[18] or temperature.[18] In this regard, the technique is similar to the path integrated imaging techniques of schlieren, interferometry, and holography, except that the measurements give a time history of the integrated index along a single line instead of a 2-D image at a single time as obtained with a pulsed imaging technique. The beam deflection technique is attractive because of its simplicity in implementation and analysis.[14] Beam deflection measurements have been used to perform electron density and gas density measurements in laser-produced plasmas[3,15,16] and other plasmas[19–22] as well as a diagnostic for laser ablation and associated density variations.[23–26]

The many components in a plasma make the interpretation of index of refraction measurements complicated.[27] When electron density n_e is well below the critical density n_c, the index of refraction for free electrons is approximately

$$n = 1 - \frac{1}{2} \frac{n_e}{n_c}. \tag{2}$$

The critical density is given by

$$n_c = \frac{\pi m_e c^2}{e^2 \lambda^2}, \tag{3}$$

where m_e is the mass of the electron, c is the speed of light, e is the charge of the electron, and λ is the wavelength of the light. Thus the index of refraction

When this work was done both authors were with Lund Institute of Technology, Physics Department, P.O. Box 118, S-221 00 Lund, Sweden; G. W. Faris is now with SRI International, Molecular Physics Laboratory, 333 Ravenswood Avenue, Menlo Park, California 94025.

Received 18 July 1990.
0003-6935/91/162212-07$05.00/0.

for electrons is less than one and varies rapidly with wavelength. This is in contrast to the index of refraction for the other components of the plasma (ions, neutral atoms, molecules, and particles), which is greater than one for visible and infrared wavelengths and, except near optical resonances, slowly varying. By using a two-wavelength technique the contributions from the electrons can be separated from the other components. In this paper we describe a two-wavelength beam deflection technique for the measurement of electron density in laser-produced plasmas.

II. Experiment

The apparatus used for our beam deflection measurements is shown in Fig. 1. To avoid the effects of background gas on the measurements, the plasma is formed in a chamber evacuated to 10^{-7} mbar. The plasma is formed by using a 250-mm lens to focus 25–50 mJ of 1.06-μm radiation from a Q-switched Nd:YAG laser (Quanta-Ray DCR) to an intensity of $\sim 10^{10}$ W/cm^2 on a rotating target. The position of the focus is moved between measurements to maintain a clean surface on the target for each measurement. Targets made of boron, graphite, silicon, iron, tantalum, and tungsten were used.

A He–Ne laser and a He–Cd laser, operating at 632.8 and 441.6 nm, respectively, were used as probe lasers. An air-cooled Ar^+ laser was used instead of the He–Cd laser for early measurements[15] but vibrations caused by the fan were found to significantly reduce the sensitivity of the measurements. The He–Ne and He–Cd lasers differ by about a factor of 2 in the index of refraction for the electrons [Eqs. (2) and (3)], and the critical densities for these wavelengths (2.78×10^{21} and 5.72×10^{21} cm^{-3} for the He–Ne and He–Cd wavelengths, respectively) are well above those found in the plasmas. Thus Eq. (2) is valid and the absorption by the electrons is very small. A dichroic mirror is used to combine the two lasers and a 500-mm lens is used to focus both beams in the plasma. The two laser spots were carefully overlapped in the plasma region to avoid systematic errors. The distance of the He–Cd laser from the dichroic mirror is varied to give focal spots of the same size (250 μm) to within 5%. Accurate overlap of the two laser beams is obtained using the two quadrant detectors. The detector at the left is used to overlap the beams at the dichroic mirror, while the detector at the right is used to overlap the beams over their lengths. The adjustment of these positions is decoupled by using a tilted optical flat (window) placed in front of the He–Ne laser. Changing the angle of the optical flat allows translation of the He–Ne beam without changing the beam's direction, while tilting the dichroic mirror allows changing the beam direction with minimal change in overlap at the mirror.

The He–Ne and He–Cd lasers used for the deflection measurements have little noise at frequencies over 10 kHz and little beam-pointing drift after being warmed up ($\sim$1 h). Thus, there is little noise on the time scales of a beam deflection measurement, which is performed over 2.5 μs. There is also little mechanical vibration at these frequencies, and although the experiments were performed on the third floor of a building, good results were obtained with the two lasers and the detector all on separate tables (of which none was an optical table). Normal optical interferometry would not be possible in these conditions. The He–Ne laser, with mirrors hard-sealed onto the tube, was particularly stable, and we have measured deflection angles to 200 nrad in a plasma when averaging 100 laser shots. This is equivalent to a variation of $\sim$13,000th of an interference fringe over the spot size of 250 μm.

For best results, the beam waists (focal spots) of the probe lasers are placed at the center of the plasma. The beam waist spot size then determines the spatial resolution, the minimum measurable deflection angle, and the maximum deflection angle measurable with good linearity. Reducing the beam waist size improves the spatial resolution until a point is reached where the resolution at the edges of the measurement region begins to be significantly degraded due to diffraction. This occurs for a Gaussian beam at a spot size given by[14]

$$w_o = \sqrt{\frac{\lambda l}{2\pi}}, \tag{4}$$

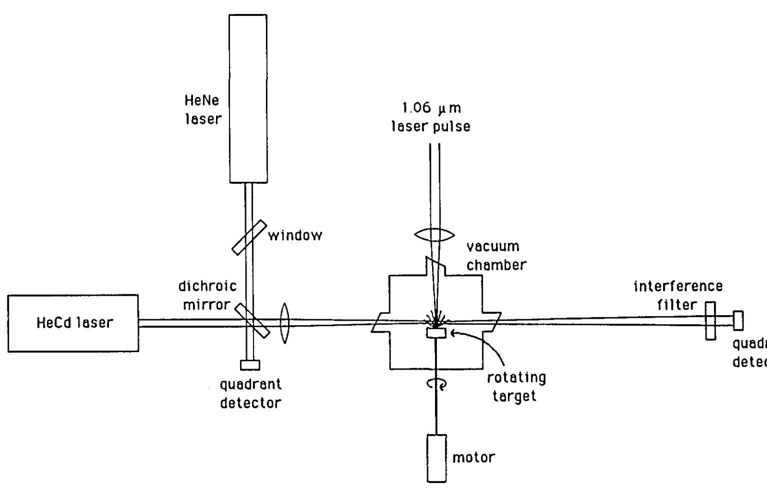

Fig. 1. Experimental arrangement for two-wavelength measurement of beam deflection angles in a laser-produced plasma.

where w_o is the $1/e^2$ beam radius of the probe intensity at the beam waist, and l is the length of the measured region. When using a segmented detector such as a split (bicell) or quadrant detector to measure deflections, the deflection signal has the form of an error function, $V_{\max}\,\mathrm{erf}(\sqrt{2}y/w_{ff})$, where $V_{\max}$ is the voltage from the entire laser beam, y is the deflection distance, and w_{ff} is the far field spot size, $w_{ff} = \lambda x/\pi w_o$, at a distance x from the focal spot. The signal is linear to within 5% for deflections up to $\sqrt{2}y/w_{ff} = 0.39$. (Although lateral detectors give linear signals over large deflections, they are too slow for measurements in laser-produced plasmas.) The maximum deflection signal size with good linearity is thus

$$\alpha_{\max} \sim \frac{0.39}{\sqrt{2\pi}}\frac{\lambda}{w_o}. \tag{5}$$

The slope of the error function signal is $dV/dy = 4V_{\max}/\sqrt{2\pi}w_{ff}$. If the limiting noise may be expressed as a voltage, $V_{\min}$, as is the case for noise from the electronics or from laser intensity fluctuations, the minimum detectable deflection is

$$\alpha_{\min} = \frac{1}{2\sqrt{2\pi}}\frac{V_{\min}}{V_{\max}}\frac{\lambda}{w_o}. \tag{6}$$

For the measurements here, focal spots of $w_o = 250\ \mu$m were used. As the measurement region in the plasma is 20 mm or less, Eq. (4) shows there is no resolution degradation. This spot size allows linear measurements up to deflection angles of 220 μrad, while the largest deflection angles we have measured in the plasmas was 300 μrad. With the 200 nrad as the smallest detectable deflection, the dynamic range is >1000. A transform lens placed between the measurement volume and the detector eliminates errors from beam displacements on traversing a sample.[14] Because of the large distance between the plasma and the detector (2.2 m), no transform lens was used. Although using a transform lens affects the spot size at the detector, it is easily shown that the maximum and minimum measurable deflections are still determined by the focal spot size in the measurement region according to Eqs. (5) and (6).

To eliminate the intense light from the Nd:YAG laser and the plasma, an interference filter is placed in front of the quadrant detector. The filter is exchanged to allow measurement of either the 632.8- or 441.6-nm beams. Two of the outputs of the quadrant detector are individually ac coupled and amplified two times each in fast amplifiers (EG&G Ortec model 574 amplifiers, 4.5 gain, 1.2-ns rise time) and input to the differential inputs of a Biomation model 8100 transient digitizer (10-ns sample time, 3 dB at 25 MHz). The transient digitizer is triggered using light from the Nd:YAG laser pulse. For all the measurements presented here, zero time corresponds to the leading edge of the Nd:YAG laser pulse, which is digitized separately on the transient digitizer. The data are transferred to an IBM AT computer for signal averaging, storage, and analysis. Typically, 100 laser shots are averaged for a beam deflection measurement. The signal detector is mounted on a micrometer-driven translation stage. By translating the detector horizontally, a calibration of detector voltage vs deflection distance is obtained for calculation of the deflection angle.

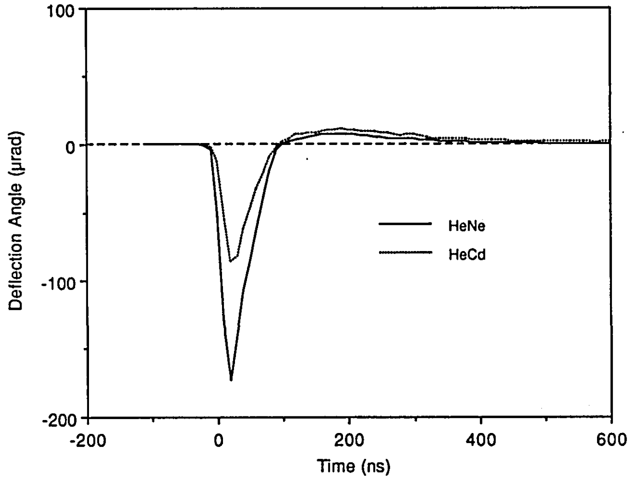

Fig. 2. Example of temporal beam deflection profile in a laser-produced plasma measured at 0.5 mm from a silicon target. The solid line corresponds to the He–Ne measurement, the dashed line is for He–Cd.

An example of a beam deflection measurement performed in a silicon plasma at a distance of 0.5 mm from the target is shown in Fig. 2. The He–Ne signal is shown as a solid line, and the He–Cd signal as a dashed line. Negative deflections correspond to deflection away from the target. From the two-wavelength measurements, the interpretation of the beam deflection measurement is straightforward. From Eqs. (2) and (3) it is apparent that the index of refraction contribution for electrons at the two wavelengths used should differ by a factor of ~2. As the deflection angle given in Eq. (1) scales linearly with the index of refraction, the deflection angles will also differ by a factor of 2. For the small deflection approximation of Eq. (1), the deflections due to electrons and the remainder of the plasma may be added. Thus the initial, negative signal in Fig. 3 is due predominantly to electrons. The later, positive part of the deflection has about equal signal sizes at the two wavelengths. Thus, this signal is primarily the result of neutral species. This positive part of the beam deflection was only present within ~1 mm from the target and was not present for the tantalum and tungsten targets. A large positive deflection was found for the He–Cd measurements with an iron target, apparently because of enhancement from the proximity of a strong resonance at 441.51 nm in Fe I (Ref. 28) to the He–Cd wavelength of 441.6 nm. The presence of the positive signal approximately correlates with the boiling points of the target material, which tends to support a delayed vaporization of the target as described by Allen.[29] The separation of the beam deflection signal into portions with dominant and minimal contributions from electrons is fortunate (this was typical for all the targets studied). In spite of the care in matching the laser beam probes, irreprodu-

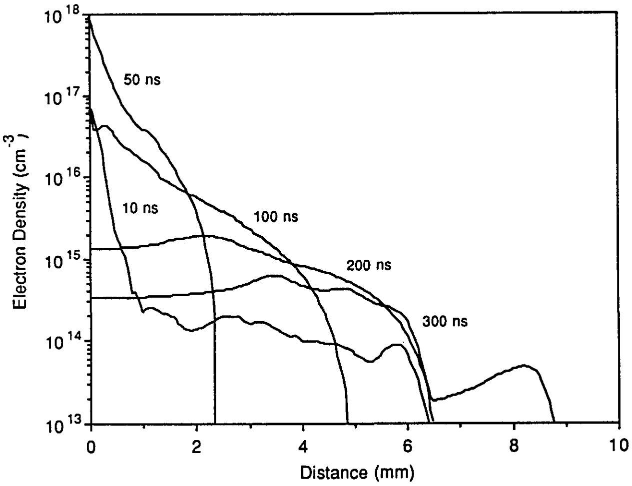

Fig. 3. Electron density profiles for a laser-produced plasma with a graphite target, reconstructed from a composite of many temporal beam deflection curves.

cibility of the plasma and, for larger distances from the target, excess noise for the He–Cd measurements did not allow separation of electron and nonelectron signals with good signal to noise. Instead, the electron density calculations below were made with the He–Ne wavelength measurements alone, and the positive signal was set to zero. The measurements with the He–Cd were used as a check for the accuracy of this simplification.

For distances less than ~500 μm from the target, absorption of the probe laser was often present, appearing as an asymmetry between the signals from the two sides of the quadrant detector. When this occurred, the two signals were digitized separately, and a single deflection signal was subsequently calculated which was corrected for the effects of absorption of the probe laser.

To accurately reconstruct the electron density in the plasma requires recording deflection curves such as that in Fig. 2 at many distances from the target. If the plasma is reproducible, these data may be taken with a single laser beam. This was done by translating both the target and focusing lens for the 1.06-μm radiation. Then, if the plasma may be approximated as spherically symmetric, the index of refraction may be calculated by using a tomographic reconstruction technique.[14] In this case, the same projection (deflection angle as a function of distance at a fixed time) is used 100 times. While the plasma is not strictly spherically symmetric, the error in the reconstructed densities is estimated to be less then a factor of 2. The result of applying this technique to beam deflection measurements in a plasma produced from a graphite target is shown in Fig. 3. The peak electron densities agree well with those measured interferometrically for comparable focused laser intensities.[2]

As the data acquisition and analysis for the reconstruction technique above are lengthy, it is of interest to examine simpler techniques to provide estimates of electron densities. If it is assumed that the plasma expansion obeys a self-similar behavior[30] with a conservation of the total number of electrons,[31] an electron density profile may be obtained using a single deflection measurement. For a self-similar expansion, we write the electron density n_e as

$$n_e(r,R) = \frac{(n_e R^3)_o}{R^3}\, \hat{n}_e\left(\frac{r}{R}\right), \tag{7}$$

where r is the distance from the pulsed laser focus, R is a variable that scales with the size of the plasma, $\hat{n}_e$ is a normalized density profile, and n_{e_o} is the peak density when $R = R_o$. Because the deflection angle scales only as the peak index of refraction,[14] the deflection angle α has the same scaling relationship as for the electron density:

$$\alpha(y,R) = \frac{(\alpha R^3)_o}{R^3}\, \hat{\alpha}\left(\frac{y}{R}\right). \tag{8}$$

The scaling variable may be written as the product of an expansion velocity v and the duration the plasma has been expanding t; $R = vt$. If velocity v is constant (this is shown to be approximately valid below), a single deflection curve, such as the one in Fig. 2, contains information on the plasma electron density at all times for a self-similar expansion. Such a curve defines $\alpha(r,R) = \alpha(r,vt)$ for r fixed and varying time t. The normalized deflection curve as a function of distance $\hat{\alpha}(r/R)$ can be recovered by multiplying the deflection curve as a function of time by t^3, where $t = 0$ should correspond to the initiation of the plasma, and then plotting the curve as a function of $1/t$. Scaling of the axes is determined by ensuring that the deflection at a given distance and time for the new curve agree with the same time and distance in the original curve. In principle, the time for the deflection curve found in this manner can be chosen arbitrarily. However, the signal to noise is best when reconstructing for times where the deflection angle in the original curve is relatively large. The results when this technique is applied, together with tomographic reconstruction for the same data used for Fig. 3, are shown in Fig. 4. The agreement with the results in Fig. 3 is quite good, except for the curve reconstructed at 10 ns. The self-similar approximation is not valid at 10 ns because the total number of electrons is still growing.

Determination of electron density profiles may be simplified further if, in addition to the assumption of self-similar behavior, it is assumed that the functional form of the electron density vs distance from the target is known. Then the deflection measurement may be used to scale the distribution. For example, if the electron density is given by a Gaussian distribution,[32] and the peak deflection measured as a function of time at a position y^* is α^*, it may be shown that the electron density is given by

$$n_e = \frac{e^2}{\sqrt{2\pi}}\, \alpha^* n_c \exp(-2r^2/y^{*2}). \tag{9}$$

This equation was used together with the data used for Figs. 3 and 4 to calculate the electron density profiles shown in Fig. 5. Electron density curves are only

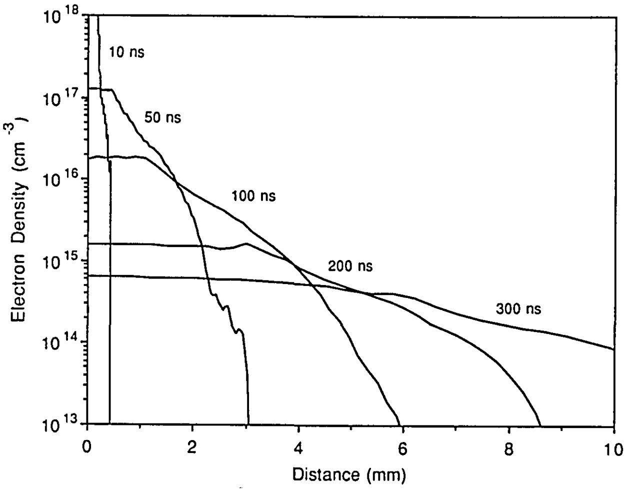

Fig. 4. Electron density profiles for a laser-produced plasma with a graphite target, reconstructed from single temporal beam deflection curves. The 10-ns profile is calculated from a measurement made at 0.5 mm from the target. The correspondences for the other times are 50 ns at 1.4 mm, 100 ns at 3.7 mm, 200 ns at 5.0mm, and 300 ns at 5.5 mm.

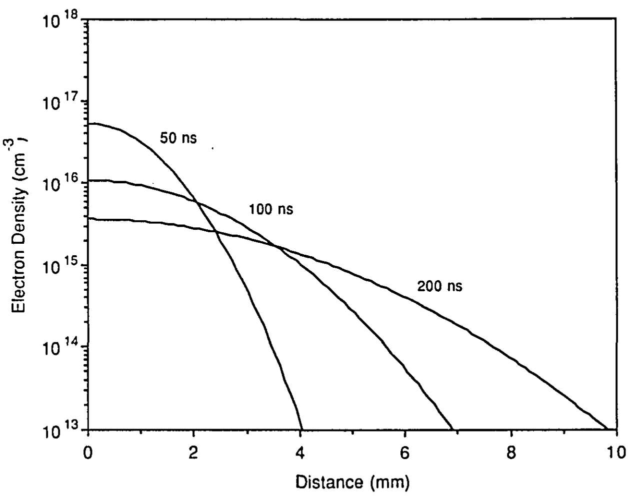

Fig. 5. Electron density profiles for a laser-produced plasma with a graphite target, calculated from peak deflection angles assuming a Gaussian density dependence.

shown for 50, 100, and 200 ns because there were no data containing peaks at earlier or later times with good signal to noise. As indicated in Eq. (10), the peak deflection for a temporal deflection curve occurs at a point where the electron density (and the deflection angle) is small compared to their peak values; this is because of the $1/R^3$ factor in Eqs. (7) and (8). The calculated electron densities shown in Fig. 5 agree fairly well with those found from the more involved techniques for Figs. 3 and 4.

Calculation of the peak electron density and spatial extent is not that sensitive to the exact functional form of the electron distribution. For example, using eleven of the twelve hypothetical electron density distributions given by Keilmann[33] (his distribution number 11 has no beam deflection peak for finite times), the peak

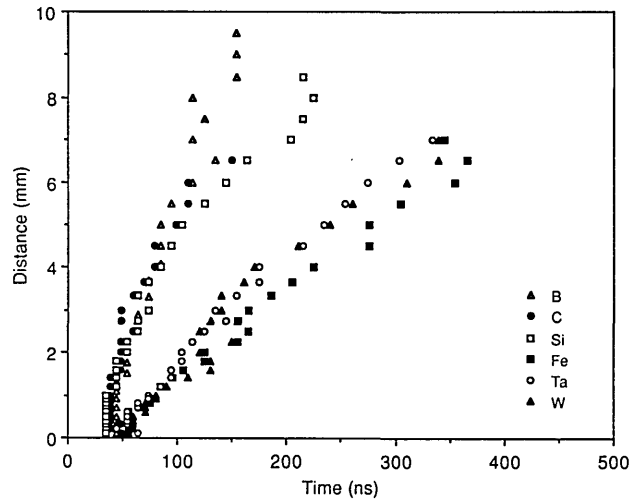

Fig. 6. Distance from the target vs time for the peak deflection angle for a number of targets.

deflection for a fixed position deflection curve occurs at a position

$$y^* = (0.915 \pm 0.06)R, \tag{10}$$

where Keilmann defines R by $\hat{n}(R) = 0.1\ \hat{n}(0)$. The peak deflection angle is given by

$$\alpha^* = (0.683 \pm 0.26)\,\frac{n_e(r = 0)}{n_c}, \tag{11}$$

where $n_e(r = 0)$ is the peak electron density at that moment.

The fixed position deflection curves allow simple determination of the expansion velocity of a laser-produced plasma. To the degree that the shape of the plasma does not change (as is true for a self-similar expansion, for example), the time for a peak deflection at a given distance determines the expansion velocity. As an example, the measurement distance as a function of the peak deflection time is shown for a variety of targets in Fig. 6. The data were taken for approximately equivalent power densities from the Nd:YAG laser. For times after ~50 ns, the velocities are about constant in the 20–100-km/s range. The corresponding ion kinetic energies we have measured are in the range of 800 eV to 1 keV for the tantalum and tungsten targets and the 200–400-eV range for the other targets. This is in agreement with the results obtained by Bykovskii *et al.*[34] using a mass spectrometer.

III. Discussion

The sensitivity of the beam deflection technique may be enhanced fairly simply. The temporal resolution was primarily limited by the large area of the quadrant detector. This could be improved by using a smaller split detector, although a faster transient digitizer would also be required. Because there is little laser noise in the measurement bandwidth, beam deflections can be measured using a very fast single element detector (up to ~50-ps rise time is available) in conjunction with a razor blade to block half of the laser beam. A collection lens can be placed between the razor blade and the detector to collect all the light which passes the razor blade onto the small detector area. If desired, the laser power can be monitored with a beam splitter and another fast detector to improve the signal to noise. Because the index of refraction is inversely proportional to the square of the detection wavelength, using infrared lasers such as laser diodes[35] for the deflection measurement enhances the sensitivity for small electron densities while still maintaining the validity of the approximation in Eq. (2).

Although the experiments described here were not successful in completely separating the contributions of electrons from the remaining plasma components, improvements in the apparatus should make this possible. By using a second dichroic mirror to separate the beams just before the detector, measurements could be taken at both wavelengths simultaneously. The relative stability of the two beams could be assured by passing both beams through a single pinhole or optical fiber and using an achromat lens to image the pinhole or fiber end into the center of the plasma.

The apparatus for beam deflection measurements in a laser-produced plasma can be very simple. We measured deflection angles close to the target by coupling the unamplified detector signal directly into an oscilloscope. Thus the minimum equipment needed is a He–Ne or similar laser, a fast photodiode, a razor blade, and an oscilloscope.

A possible method to measure fixed time beam deflection curves might be to use a differential interferometer. Reference 36 describes the similarity between differential interferometer measurements and beam deflection measurements as well as a simple differential interferometer with tunable sensitivity that would be well suited for laser plasma measurements. Time resolution could be obtained by using a pulsed laser or by using a diode array with a gated image intensifier.

We have applied a two-color beam deflection technique to the measurement of the electron density in laser-produced plasmas. The rapid time scales of the plasma allow reduced stability requirements and low noise. Although the reproducibility of the measurements did not permit complete separation of the contribution of the electrons to the beam deflections (or index of refraction) from that of the ions and neutrals, the two-color technique established that the earlier peak consisted almost entirely of electrons and that the later peak had little electron contribution. Several techniques for reconstruction of the electron density were compared. These varied from tomographic reconstruction of data from stacked fixed position beam deflection curves (with uncertainty of less than a factor of 2) to simple estimates based on the peak deflection angles which yield uncertainty of <1 order of magnitude. The technique allows straightforward measurement of the expansion velocity of the leading edge of the plasma.

This work was supported by the National Swedish Board for Technical Development and the National Science Foundation. We would like to acknowledge helpful conversations with Sune Svanberg, Hans Lundberg, Anders Persson, and Ake Bergsquist.

References

1. P. K. Carroll and E. T. Kennedy, "Laser-Produced Plasmas," Contemp. Phys. **22**, 61–96 (1981).
2. T. P. Hughes, *Plasmas and Laser Light* (Hilger, Bristol, 1975).
3. H. Bergstrom, G. W. Faris, H. Hallstadius, H. Lundberg, A. Persson, and C.-G. Wahlstrom, "Radiative Lifetime and Hyperfine-Structure Studies on Laser-Evaporated Boron," Z. Phys. D **8**, 17–23 (1988).
4. R. A. Lacy, A. C. Nilsson, R. L. Byer, W. T. Silfvast, O. R. Wood II, and S. Svanberg, "Photoionization-Pumped Gain at 185 nm in a Laser-Ablated Indium Plasma," J. Opt. Soc. Am. B **6**, 1209–1216 (1989).
5. J. B. Hopkins, P. R. R. Langridge-Smith, M. D. Morse, and R. E. Smalley, "Supersonic Metal Cluster Beams of Refractory Metals: Spectral Investigations of Ultracold Mo_2," J. Chem. Phys. **78**, 1627–1637 (1983).
6. M. L. Bortz and R. H. French, "Optical Reflectivity Measurements Using a Laser Plasma Light Source," Appl. Phys. Lett. **55**, 1955–1957 (1989).
7. M. M. Murnane, H. C. Kapteyn, and R. W. Falcone, "High Density Plasmas Produced by Ultrafast Laser Pulses," Phys. Rev. Lett. **62**, 155–158 (1989).
8. J. A. Trail and R. L. Byer, "Compact Scanning Soft-X-Ray Microscope Using a Laser-Produced Plasma Source and Normal-Incidence Multilayer Mirrors," Opt. Lett. **14**, 539–541 (1989).
9. P. Gohil, H. Kapoor, D. Ma, M. C. Pekerar, T. J. McIlrath, and M. L. Ginter, "Soft X-Ray Lithography Using Radiation from Laser-Produced Plasmas," Appl. Opt. **24**, 2024–2027 (1985).
10. S. Maxon *et al.*, "Calculation for Ni-Like Soft X-Ray Lasers: Optimization for W (43.1 Å)," Phys. Rev. Lett. **63**, 236–239 (1989).
11. A. Richter, H.-J. Scheibe, W. Pompe, K.-W. Brzezinka, and I. Muhling, "About the Structure and Bonding of Laser Generated Carbon Films by Raman and Electron Energy Loss Spectroscopy," J. Non-Cryst. Solids **88**, 131–144 (1986); C. B. Collins, F. Davanloo, E. M. Juengerman, W. R. Osborn, and D. R. Jander, "Laser Plasma Source of Amorphic Diamond," Appl. Phys. Lett. **54**, 216–218 (1989).
12. D. Dijkkamp *et al.*, "Preparation of Y–Ba–Cu Oxide Superconductor Thin Films Using Pulsed Laser Evaporation from High T_c Bulk Material," Appl. Phys. Lett. **51**, 619–621 (1987); M. J. Ferrari *et al.*, "Low Magnetic Flux Noise Observed in Laser-Deposited *In Situ* Films of $YB_2Cu_3O_y$ and Implications for High-T_c SQUIDs," Nature (London) **341**, 723–725 (1989).
13. R. Srinivasan and V. Mayne-Banton, "Self-Developing Photoetching of Poly(ethylene Terephthalate) Films by Far-Ultraviolet Excimer Laser Radiation," Appl. Phys. Lett. **41**, 576–578 (1982); S. Lazare and V. Granier, "Excimer Laser Light Induced Ablation and Reactions at Polymer Surfaces as Measured with a Quartz-Crystal Microbalance," J. Appl. Phys. **63**, 2110–2115 (1988).
14. G. W. Faris and R. L. Byer, "Three-Dimensional Beam-Deflection Optical Tomography of a Supersonic Jet," Appl. Opt. **27**, 5202–5212 (1988).
15. H. Bergstrom, G. Faris, H. Hallstadius, H. Lundberg, A. Persson, and C.-G. Wahlstrom, "Spectroscopy on Laser-Evaporated Boron and Carbon," in *Technical Digest, Eighth International Conference on Laser Spectroscopy*, Are, Sweden (22–26 June 1987).
16. C. L. Enloe, R. M. Gilgenbach, and J. S. Meachum, "Fast, Sensitive Laser Deflection System Suitable for Transient Plasma Analysis," Rev. Sci. Instrum. **58**, 1597–1600 (1987).

17. G. W. Faris and R. L. Byer, "Quantitative Three-Dimensional Optical Tomographic Imaging of Supersonic Flows," Science **238**, 1700–1702 (1987).
18. G. W. Faris and R. L. Byer, "Beam-Deflection Optical Tomography of a Flame," Opt. Lett. **12**, 155–157 (1987).
19. I. C. Potter, I. S. Falconer, and W. I. B. Smith, "Measurement of the Electron Density Distribution in Plasmas from the Bending of a Gas Laser Beam," J. Phys. E **5**, 910–914 (1972).
20. P. W. Schreiber, A. M. Hunter II, and D. R. Smith, Jr., "The Determination of Plasma Electron Density from Refraction Measurements," Plasma Phys. **15**, 635–646 (1973).
21. H. Schmidt and B. Ruckle, "Beam Deviation Method as a Diagnostic Tool for the Plasma Focus," Appl. Opt. **17**, 1275–1279 (1978).
22. M. A. Greenspan and K. V. Reddy, "A Laser Deflection Technique for Sensitive Measurements of a Reduced-Density Channel in Neutral Gas," Appl. Phys. Lett. **40**, 576–578 (1982).
23. J. M. Green, W. T. Silfvast, and O. R. Wood II, "Evolution of a CO_2-Laser-Produced Cadmium Plasma," J. Appl. Phys. **48**, 2753–2761 (1977).
24. G. Koren, "Observation of Shock Waves and Cooling Waves in the Laser Ablation of Kapton Films in Air," Appl. Phys. Lett. **51**, 569–571 (1987).
25. S. Petzoldt, A. P. Elg, M. Reighling, J. Reif, and E. Matthias, "Surface Laser Damage Thresholds Determined by Photoacoustic Deflection," Appl. Phys. Lett. **53**, 2005–2007 (1988).
26. J. A. Sell, D. M. Heffelfinger, P. Vantzek, and R. M. Gilgenbach, "Laser Beam Deflection as a Probe of Laser Ablation of Materials," Appl. Phys. Lett. **55**, 2435–2437 (1989).
27. F. C. Jahoda and G. A. Sawyer, "Optical Refractivity of Plasmas," in *Plasma Physics* R. H. Lovberg and H. R. Griem, Eds. (Academic, New York, 1971), Part B, Vol. 9, pp. 1–48.
28. W. L. Wiese and G. A. Martin, "Atomic Transition Probabilities," in *Handbook of Chemistry and Physics*, R. C. Weast and M. J. Astle, Eds. (CRC Press, West Palm Beach, FL, 1978), pp. 112–140.
29. F. J. Allen, "Production of High-Energy Ions in Laser-Produced Plasmas," J. Appl. Phys. **43**, 2169–2175 (1972).
30. A. V. Gurevich, L. V. Pariiskaya, and L. P. Pitaevskii, "Self-Similar Motion of a Rarefied Plasma," Sov. Phys. JETP **22**, 449–454 (1966); P. Mora, "Self-Similar Expansion of a Plasma into a Vacuum," Phys. Fluids **22**, 2300–2304 (1979).
31. P. T. Rumsby and J. W. M. Paul, "Temperature and Density of an Expanding Laser-Produced Plasma," Plasma Phys. **16**, 247–260 (1974).
32. G. J. Tallents, "On the Fitting of Displaced Maxwellians to Laser-Produced Plasma Ion Velocity Distributions," Opt. Commun. **37**, 108–112 (1981).
33. F. Keilmann, "An Infrared Schlieren Interferometer for Measuring Electron Density Profiles," Plasma Phys. **14**, 111–122 (1972).
34. Y. A. Bykovskii, V. G. Degtyarev, N. N. Degtyarenko, V. F. Elesin, I. D. Laptev, and V. N. Nevolin, "Ion Energies in a Laser-Produced Plasma," Sov. Phys. Tech. Phys. **17**, 517–520 (1972).
35. J. Pawliszyn, "LEDs and Laser Diodes in Schlieren Optics Methods," Rev. Sci. Instrum. **58**, 245–248 (1987).
36. G. W. Faris and H. M. Hertz, "Tunable Differential Interferometer for Optical Tomography," Appl. Opt. **28**, 4662–4667 (1989).